



CFD Simulation of flow through pipe fittings

Internship Report
CFD-FOSSEE Team
Indian Institute of Technology Bombay

Prepared by
Mukund S
BMS College of Engineering, Banglore

Under the supervision of
Prof. Manaswita Bose



INDIAN INSTITUTE OF TECHNOLOGY BOMBAY



ACKNOWLEDGEMENT

The following report was created as a part of FOSSEE semester long internship and I would like to thank FOSSEE, Indian Institute of Technology, Bombay for giving me this opportunity.

I would like to thank my project guide Prof. Manaswita Bose, Mentors Mr. Divyesh Variya and Mr. Ashley Melvin for the support in carrying out simulations through out the internship. I would also like to thank project manager Ms. Swetha Manian for giving me this opportunity.

I would like to extend my gratitude to Head, Department of Energy Science and Engineering, Indian Institute of Technology Bombay for giving the permission to use experimental data for validation and Swapnil Raut for helping with details and support.

Mukund S
BMS College of Engineering, Bangalore
Date: September 1, 2021

Contents

I Case Study 2: Flow through sudden expansion and contraction	1
1 Introduction	2
1.1 Aim	2
1.2 Theory	2
1.2.1 Major Losses	2
1.2.2 Minor Losses	3
1.3 Problem Statement	4
1.4 Schematic Diagram	5
2 OpenFOAM base case	6
2.1 pitzDaily	6
2.1.1 Folder Structure	6
2.2 Solver	7
2.2.1 Turbulence Model	8
3 OpenFOAM Case Modifications	9
3.1 Pre-processing	9
3.2 Boundary conditions	10
3.3 Physical properties	11
3.4 fvSchemes & fvSolution	11
3.5 Control parameters	11
3.6 Post-processing	11



4	Results	13
4.1	Numerical Results	13
4.1.1	Sudden Expansion	13
4.1.2	Sudden Contraction	17
4.2	Experimental Results	21
4.3	Result comparison	24
4.3.1	Sudden Expansion	24
4.3.2	Sudden Contraction	25
5	Conclusion	29

List of Figures

1.1	Sudden Expansion?	4
1.2	Sudden Contraction?	4
1.3	Schematic layout of pipe network with fittings?	5
1.4	Axisymmetric Geometry of sudden expansion	5
1.5	Axisymmetric Geometry of sudden contraction	5
4.1	Pressure contour	13
4.2	Velocity contour	14
4.3	Velocity contour for higher Reynolds number	15
4.4	Pressure contour for higher Reynolds number	16
4.5	Velocity contour for lower Reynolds number	16
4.6	Pressure contour for lower Reynolds number	16
4.7	Streamlines with Velocity contour	17
4.8	Streamlines with Velocity contour for Higher Reynolds number	18
4.9	Streamlines with Velocity contour for Lower Reynolds number	18
4.10	Pressure Distribution along the length	19
4.11	Velocity Distribution along the length	19
4.12	Vector plot for sudden expansion	20
4.13	Vector plot for sudden expansion (High Reynolds number)	20
4.14	Vector plot for sudden expansion (Low Reynolds number)	20
4.15	Pressure contour	21
4.16	Velocity contour	21
4.17	Pressure contour for Higher Reynolds number	21
4.18	Velocity contour for Higher Reynolds number	22
4.19	Pressure contour for Lower Reynolds number	22
4.20	Velocity contour for Lower Reynolds number	22



4.21	Streamlines with Velocity contour	23
4.22	Streamlines with Velocity contour for Higher Reynolds number . . .	23
4.23	Streamlines with Velocity contour for Lower Reynolds number . . .	24
4.24	Pressure Distribution along the length	24
4.25	Velocity Distribution along the length	25
4.26	Vector plot for sudden contraction	25
4.27	Vector plot for sudden contraction (High Reynolds number)	26
4.28	Vector plot for sudden contraction (Low Reynolds number)	26

List of Tables

2.1	Folder contents	7
3.1	Boundary conditions	10
4.1	Experimental and CFD results for sudden expansion	27
4.2	Experimental and CFD results for sudden expansion	28

Part I

Case Study 2: Flow through sudden expansion and contraction

Chapter 1

Introduction

1.1 Aim

The aim of this case study was to determine the minor loss factor of sudden expansion and contraction of pipes through CFD method. OpenFOAM version 1912 was used for carrying out the simulation. Further, the velocity and pressure contours of the flow were studied. The study was performed for a 2-D incompressible flow with water as the working fluid, simpleFoam steady state solver was used and $\kappa\text{-}\epsilon$ RANS model was adopted to simulate the turbulent flow. The results were viewed in ParaView 5.7.0

1.2 Theory

The resistance to flow in a pipe network causes loss in the pressure head along the flow. The overall head loss across a pipe network consists of the following:

- Major losses
- Minor losses

1.2.1 Major Losses

Major losses refer to the losses in pressure head of the flow due to friction effects. Such losses can be evaluated by using the Darcy-Weisbach equation:

$$h_{major} = f \frac{Lv^2}{2gD} \quad (1.1)$$



where f is the Darcy friction factor, L is the length of the pipe segment, v is the flow velocity, D is the diameter of the pipe segment, and g is acceleration due to gravity. Equation 1.1 is valid for any fully developed, steady and incompressible flow. The friction factor f can be calculated by the following empirical formula, known as the Blasius formula, valid for turbulent flow in smooth pipes with $Re_D < 10^5$:

$$f = 0.316Re_D^{-0.25} \quad (1.2)$$

1.2.2 Minor Losses

In a pipe network, the presence of pipe fittings such as bends, elbows, valves, sudden expansion or contraction causes localized loss in pressure head. Such losses are termed as minor losses. Minor losses are expressed using the following equation:

$$h_{minor} = K \frac{v^2}{2g} \quad (1.3)$$

where K is called the Loss Coefficient of the pipe fitting under consideration. Minor losses are also expressed in terms of the equivalent length of a straight pipe (L_{eq}) that would cause the same head loss as the fitting under consideration:

$$h_{minor} = K \frac{v^2}{2g} = f \frac{L_{eq} v^2}{2gD} \quad (1.4)$$

$$L_{eq} = K \frac{D}{f} \quad (1.5)$$

In the present study, we shall determine the head losses across sudden enlargement and sudden contraction. Loss of head due to sudden enlargement: This is the energy loss due to sudden enlargement. Sudden enlargement in the diameter of pipe results in the formation of eddies in the flow at the corners of the enlarged pipe 1.1. This results in the loss of head across the fitting. Loss of head due to sudden contraction: This is the energy loss due to sudden contraction. In reality, the head loss does not take place due to the sudden contraction but due to the sudden enlargement, which takes place just after vena-contracta 1.2.?? Figure 1.3 shows the schematic layout of the pipe network to be used in the present study.

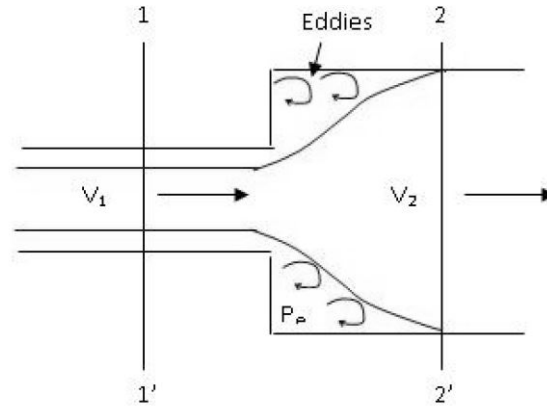


Figure 1.1: Sudden Expansion?

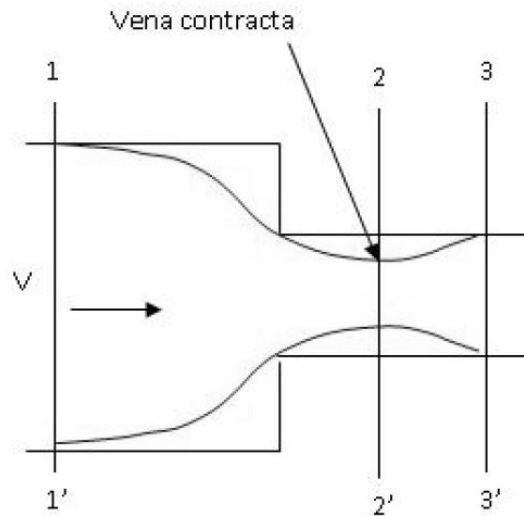


Figure 1.2: Sudden Contraction?

1.3 Problem Statement

The primary objective of the case study is to simulate turbulent flow through a sudden expansion and contraction case and later calculate the minor loss factors using the CFD result and compare it with the experimental or analytical results. The dimensions of the pipe fittings are considered from the lab manual. The simulations were conducted for 17 different cases with Reynolds number varying from the range of 6000 to 20000. To study this turbulent flow, simpleFoam solver is used.

Chapter 2

OpenFOAM base case

2.1 pitzDaily

The base case considered for the simulation of the orifice meter is the pitzDaily case. This case can be found under the incompressible section, simpleFoam subsection. The directory for this is

\OpenFOAM-v1912\tutorials\incompressible\simpleFoam\pitzDaily.

Based on the experimental work of Pitz and Daily (1981). It features a backward facing step. Such a “classic” case is instructive for comparing different turbulence models with respect to the size and shape of the recirculation zone[[internet reference](#)]. pitzDaily introduces the following concepts for the first time:

- Mesh creation using blockMesh and also mesh grading capability
- Turbulent steady flow.

2.1.1 Folder Structure

Any case file in OpenFOAM has three folders, called the 0, constant and the system. The constant contains coefficient values that will be used in equations and also things which will remain constant like the mesh, material properties, environmental constants which the solver uses, the 0 folder contains the initial and boundary conditions, and the system folder contains the configuration files for the mesh and also how the solver will be executed, schemes and methods to use and controls for the simulation.



Table 2.1: Folder contents

Directories	Constant	0	System
Sub-directories	transportProperties turbulenceProperties polyMesh	U p nut epsilon k	blockMeshDict fvSchemes fvSolution

2.2 Solver

OpenFOAM or Open-source Field Operation And Manipulation is an open-source C++ tool used for solving continuum mechanics problems, with a focus on Finite Volume Method (FVM). The software package includes solver codes for different kinds of transport phenomena, varying from simple laplacian solver called laplacianFoam to complex multiphase flow, compressible flow, heat transfer, incompressible flow, and many more. The flagship solver and most commonly used solver is simpleFoam. simpleFoam is a steady-state solver for incompressible, turbulent flow. It utilizes the SIMPLE (Semi-Implicit Method for Pressure Linked Equations) algorithm. It is an approximation of the velocity field which is obtained by solving the momentum equation. The pressure gradient term is calculated using the pressure distribution from the previous iteration or an initial guess. The pressure equation is formulated and solved to obtain the new pressure distribution. Velocities are corrected and a new set of conservative fluxes is calculated. The solver used for this case study is simpleFoam, it employs SIMPLE algorithm. The case study considered is a steady state, incompressible, three-dimensional flow. The set of Navier Stokes equations governing the flow is given below.

The continuity equation is given as,

$$\nabla \cdot \vec{u} = 0 \quad (2.1)$$

The momentum equation is given as.

$$\frac{\partial \vec{u}}{\partial t} + \nabla \cdot [\vec{u}\vec{u}] = -\frac{1}{\rho} \nabla p + \nu \nabla^2 \vec{u} \quad (2.2)$$

Where, \vec{u} is velocity, p-pressure; ν is kinematic viscosity The discretized momentum equation and pressure correction equation are solved implicitly, where the



velocity correction is solved explicitly. This is the reason why it is called "Semi-Implicit Method".

2.2.1 Turbulence Model

The turbulence model considered for the simulation is κ - ϵ RANS model. κ - ϵ model solves two additional equations, for turbulent kinematic energy κ and rate of dissipation of turbulence energy ϵ . It performs poorly for complex flows involving severe pressure gradient, separation, strong streamline curvature. Suitable for initial iterations, initial screening of alternative designs, and parametric studies. Can be only used with wall functions. The equations for the κ - ϵ RANS model is below,

$$\frac{\partial(p\kappa)}{\partial t} + \frac{\partial(p\kappa u_i)}{\partial x_i} = \frac{\partial}{\partial x_j} \left[\frac{\mu_t}{\sigma_\kappa} \frac{\partial \kappa}{\partial x_j} \right] + 2\mu_t E_{ij} E_{ij} - \rho \epsilon \quad (2.3)$$

$$\frac{\partial(p\epsilon)}{\partial t} + \frac{\partial(p\epsilon u_i)}{\partial x_i} = \frac{\partial}{\partial x_j} \left[\frac{\mu_t}{\sigma_\epsilon} \frac{\partial \epsilon}{\partial x_j} \right] + C_{1\epsilon} \frac{\epsilon}{\kappa} 2\mu_t E_{ij} E_{ij} - C_{2\epsilon} \rho \frac{\epsilon^2}{\kappa} \quad (2.4)$$

where u_i represents velocity component in corresponding direction, E_{ij} represents component of rate of deformation, and μ_t represents eddy viscosity. The default value of model coefficients $C_{1\epsilon}$, $C_{2\epsilon}$, σ_κ , σ_ϵ and C_μ have been used.

Chapter 3

OpenFOAM Case Modifications

Using the pitzDaily case, modifications were made with the geometry, the mesh used, boundary conditions applied to it, and the control parameters which are going to be explained further in the below sections.

3.1 Pre-processing

The models for both the case was created using the dimensions from the manual provided ?. To simplify the calculations, an axisymmetric wedge was created. In OpenFOAM to make the axisymmetric wedge the angle should be 5 degrees. The upstream length and downstream length was taken to be 400mm and axis along Z direction for both the cases.

The mesh and geometry was created using the blockMesh utility. The blockMeshDict file from the base case was modified to create the axisymmetric model of the sudden expansion and contraction geometry. convertToMeters, the very first line of blockMeshDict file was changed, by default the units used in OpenFOAM are in meters. Since the geometry is in millimetres a conversion factor from meters to millimetres was used, replacing 0.01 to 0.001.

The co-ordinates of the geometry are entered in the vertices column of the file. It is entered as x, y, and z coordinate values. X represents the radial distance; Y represents the angular axis and Z represents the axial length of the geometry for sudden expansion case and Y represents the radial distance; X represents the angular axis and Z represents the axial length of the geometry for sudden contraction case. Therefore the coordinate axis can be obtained by simple trigonometric



formula of $\tan = \frac{\text{Oppositeside}}{\text{adjacentside}}$. The geometry is divided into blocks for Meshing purposes. There are totally 3 blocks. It was made using hexahedral blocks with simplegrading 1 in all directions to make sure the nearest cell thickness near the wall region would be in the log-law region for sudden expansion case and for the sudden contraction case, the expansion ratio was chosen (0.015), to have refinement near the walls so that the nearest cell thickness near the wall region would be in the viscous sub-layer region. In the axisymmetric geometry, the front, back panels, and the axis are additional boundaries. Proper patchfields are assigned to them, for the front and back panels, boundary patch assigned is wedge and for the axis it is given as empty. Using the blockMesh utility, the mesh was generated and with checkMesh, the quality of the mesh was determined. For the sudden expansion case, the $y+$ value was selected in the log-law region as suggested in ? and for sudden contraction the $y+$ was considered in the viscous sublayer.

3.2 Boundary conditions

The initial and boundary conditions are included in the 0 folder as k, epsilon, nut,p, and U. The boundary conditions are summarised in the Table 3.1 for both the cases. In all the files in 0 folder, the axis, front_back_pos and front_back_neg were given

Table 3.1: Boundary conditions

	inlet	outlet	wall
epsilon	fixedValue	zeroGradient	epsilonWallFunction
k	fixedValue	zeroGradient	kqRWallFunction
nut	calculated	calculated	nutkWallFunction
p	zeroGradient	fixedValue	zeroGradient
U	fixedValue	zeroGradient	noSlip

the boundary condition of empty, wedge and wedge respectively. The value for κ and ϵ were determined using the below equations

$$\kappa = \frac{3}{2}(uI)^2 \quad (3.1)$$

$$\epsilon = \frac{C_{\mu}^{0.75} \kappa^{1.5}}{0.07l} \quad (3.2)$$



where u is the free stream velocity, I is the turbulence intensity, C_μ is the model coefficient, l is the characteristic length.

3.3 Physical properties

The working fluid for both the simulation was water. The density considered was 1000 kg/m^3 , with a kinematic viscosity of $1 \times 10^{-06} \text{ m}^2/\text{s}$. So the value in the transportProperties file was changed to 1×10^{-06} from 1×10^{-05} and the transportModel remained as it is to Newtonian.

3.4 fvSchemes & fvSolution

fvSchemes and fvSolutions are found under the constant folder. fvSolution directory contains equation solvers, algorithms and tolerances. No changes were done to this file, the tolerances for the residuals were pre-set to a value of $1\text{e-}05$ and it was not changed. The numerical schemes for the simulation are entered in the fvSchemes dictionary. No changes were made in this file directory.

3.5 Control parameters

The OpenFOAM solvers begin all runs by setting up a database. The database controls I/O and, since output of data is usually requested at intervals of time during the run, time is an inextricable part of the database. The controlDict dictionary sets input parameters essential for the creation of the database. Here the endTime was changed to 10000, i.e., maximum iterations were 10000. startTime was 0 and writeInterval was set to every 100 iterations with 1 as deltaT as it was a steady state analysis.

3.6 Post-processing

After the simulation has been completed, the results were viewed in ParaView. To do this, first the results obtained were converted into viewable file using the command `touch suitable_file_name.foam`. A file with .foam extension was created. In this file, the results was viewed, the various contours of the solution was visualised,



streamlines were plotted and the data were analysed with the in-built plotting options available.

Chapter 4

Results

Steady state simulations were performed using SIMPLE algorithm for $\kappa - \epsilon$ RANS model. The obtained CFD results have been compared with the experimental results for the coefficient of discharge. Post-processing was done using paraview.

4.1 Numerical Results

The post-processing of the simulation was done in ParaView for both the cases each having 17 simulations. The numerical results are further discussed below.

4.1.1 Sudden Expansion

The velocity and pressure contours obtained by the simulations are shown in Figure 4.1 and 4.2. From the pressure contour we can see that there is a gradual decrease in pressure due to the frictional losses at the inlet.

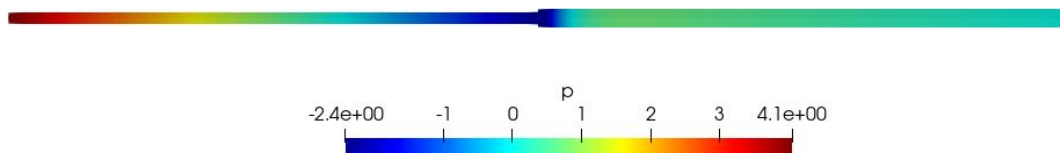


Figure 4.1: Pressure contour

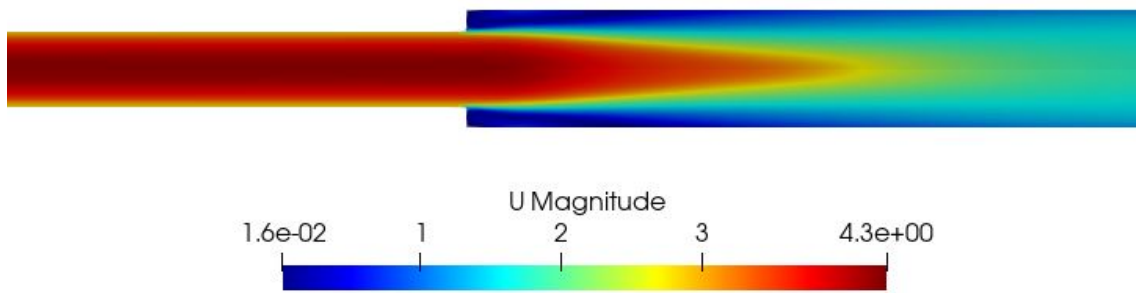


Figure 4.2: Velocity contour

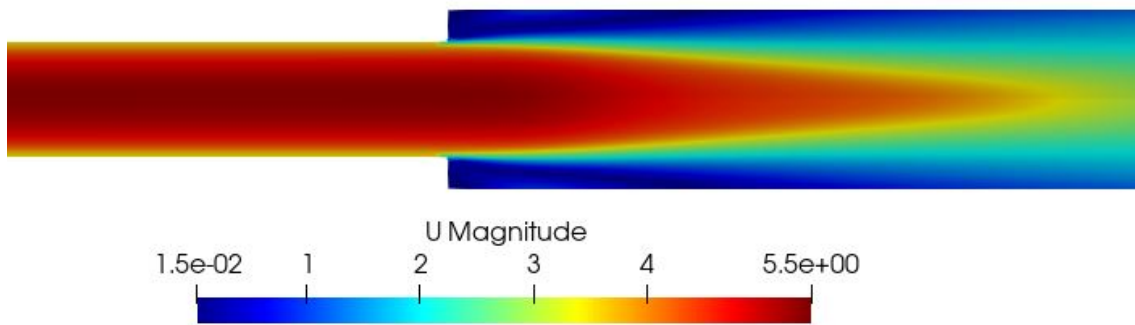


Figure 4.3: Velocity contour for higher Reynolds number

As the fluid reaches the transitional section, the fluid is decelerated in the enlarged pipe area and there occurs a sudden rise in pressure?. In the velocity contour it is seen that right after the transitional region, eddies are formed. The evolution

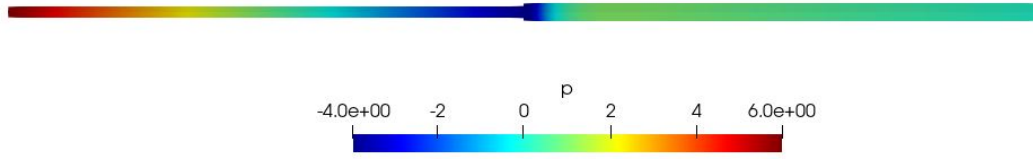


Figure 4.4: Pressure contour for higher Reynolds number

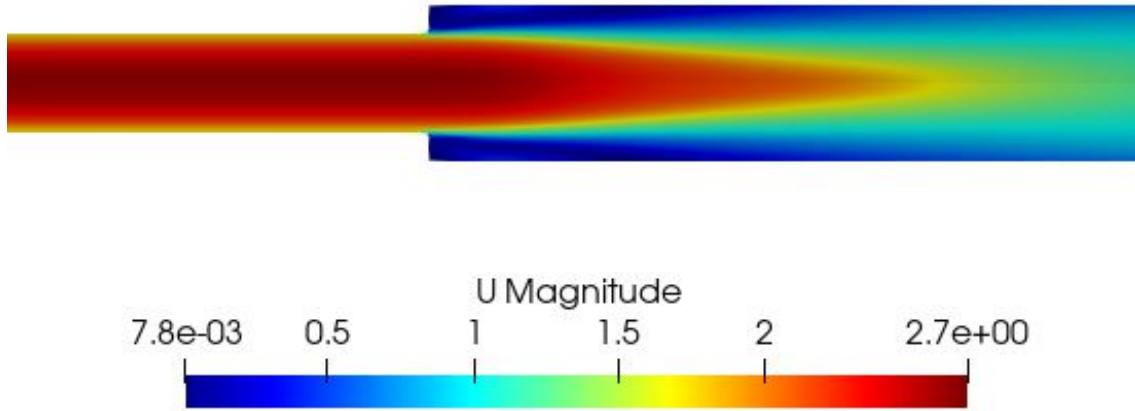


Figure 4.5: Velocity contour for lower Reynolds number

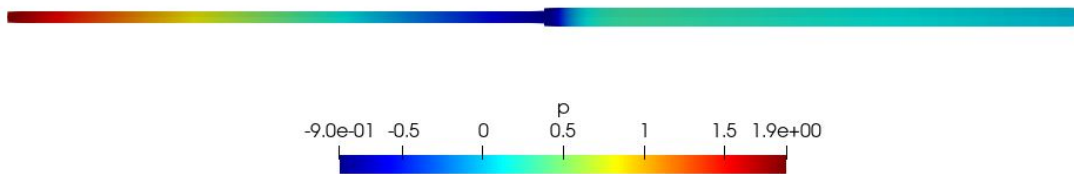


Figure 4.6: Pressure contour for lower Reynolds number

of the solution is plotted for both pressure and velocity. Furthermore, pressure and velocity contours for lower and higher Reynolds number are plotted which



are shown in Figure 4.3-4.6. This can be further visualised through the streamlines plotted for this case as shown in Figure 4.7. The re-circulation region right

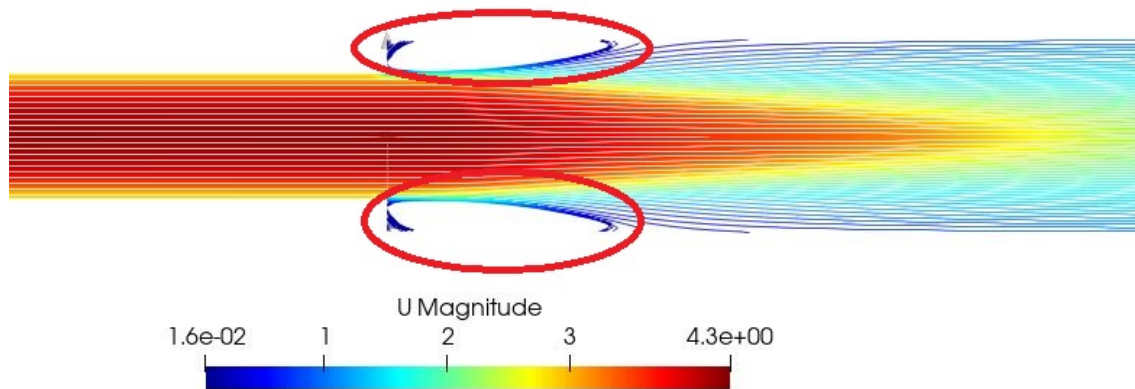


Figure 4.7: Streamlines with Velocity contour

after the expansion can be seen in the streamline. Re-circulation region is circled in red colour. Streamlines for higher and lower Reynolds number are also plotted and is shown in Figure 4.8 and Figure 4.9 respectively. Pressure and velocity distribution along the length of the pipe is plotted as shown in Figure 4.10 and Figure 4.11. From these graphs we see that right after the change in cross-sectional area, there is a sudden increase in the pressure and drop in the velocity around the length of 0.4-0.45m. The pressure change at the expansion plane (ΔP_e) is obtained by extrapolating the computed pressure profiles upstream and downstream of the pipe expansion (in the region of fully developed pipe flow) to the expansion plane. Vector plots for the different Reynolds number is shown in Figure 4.12-4.14.

4.1.2 Sudden Contraction

Contours for pressure and velocity are shown in Figure 4.15 and Figure 4.16. From the pressure contour it can be seen that at a few distance from the entrance of the sudden contraction, there is a high pressure region and after the change in geometry, the pressure value decreases suddenly and then gradually to zero. In the

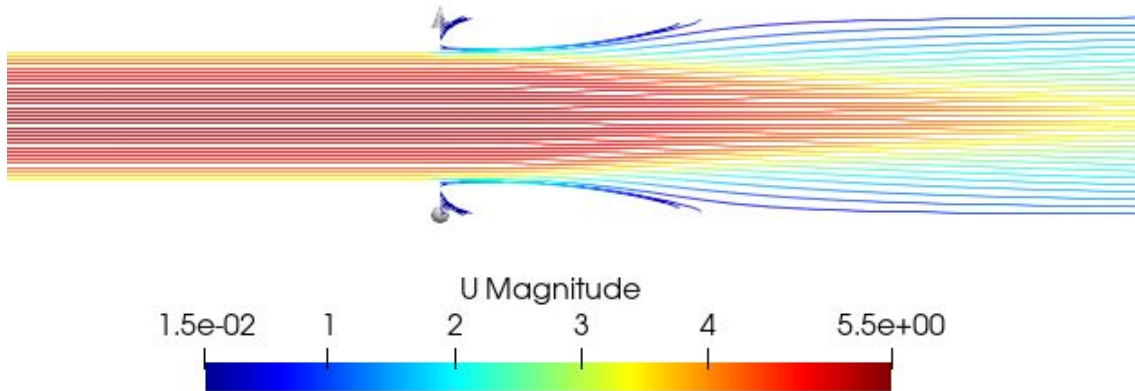


Figure 4.8: Streamlines with Velocity contour for Higher Reynolds number

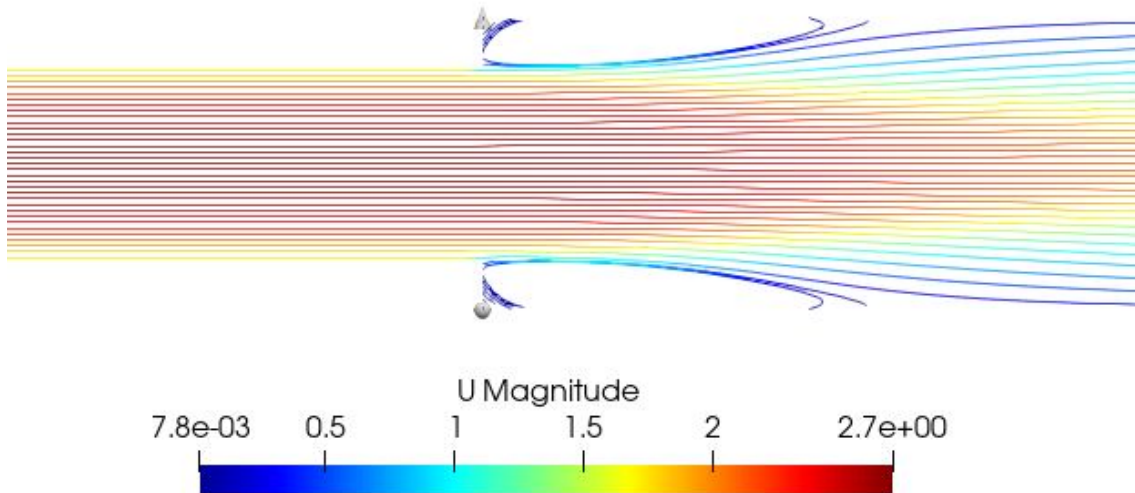


Figure 4.9: Streamlines with Velocity contour for Lower Reynolds number

velocity contour, the magnitude of the velocity is low before the sudden contraction is approached, at the entrance there's an increase in the velocity and after the

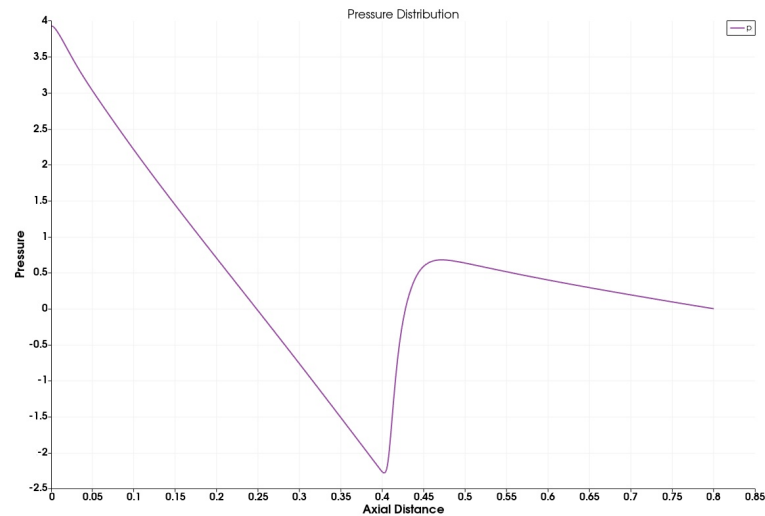


Figure 4.10: Pressure Distribution along the length

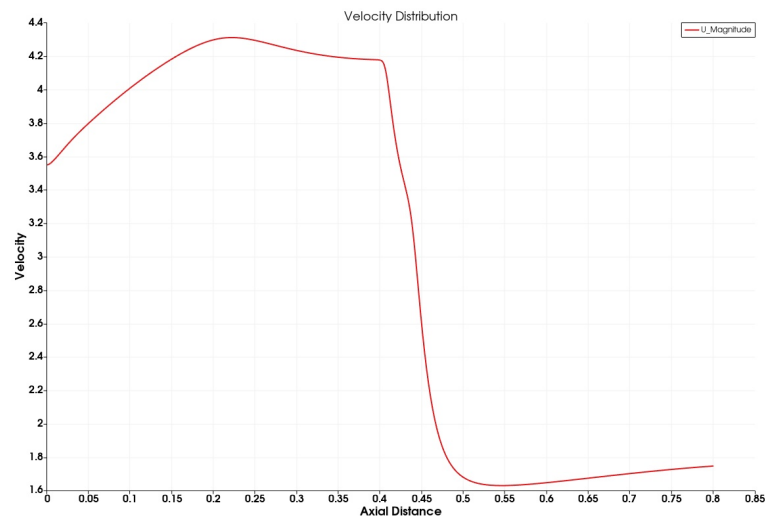


Figure 4.11: Velocity Distribution along the length

change in geometry, the value saturates. Velocity and pressure contours for higher and lower Reynolds number are also plotted to get a better understanding of the flow for various Reynolds number regime and is shown in Figure 4.17-4.20

To better understand the flow, streamlines were plotted and is shown in Figure 4.21 From these streamlines we can see, the fluid converges before the entrance and a region of vena-contracta is forming few metres right after the entrance. Streamlines are also plotted for higher and lower Reynolds number, as shown in Figure 4.22 and 4.23. Pressure and velocity distributions were plotted along the length

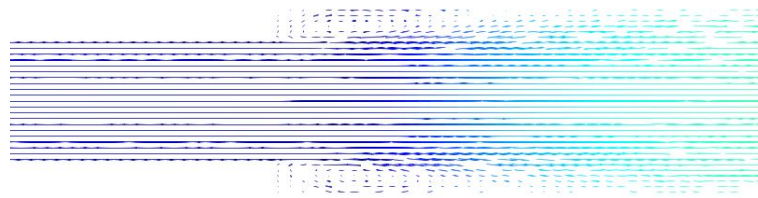


Figure 4.12: Vector plot for sudden expansion

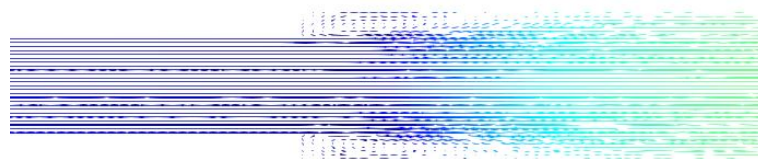


Figure 4.13: Vector plot for sudden expansion (High Reynolds number)

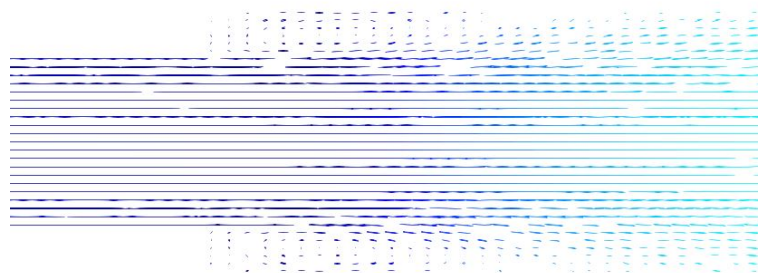


Figure 4.14: Vector plot for sudden expansion (Low Reynolds number)

of the pipe and is shown in Figure 4.24 and Figure 4.25. The plots obtained show the same physics that was seen in the pressure and velocity contours. Vector plots have also been plotted to get a better understanding for various Reynolds number. They are shown in Figure 4.26-4.28.

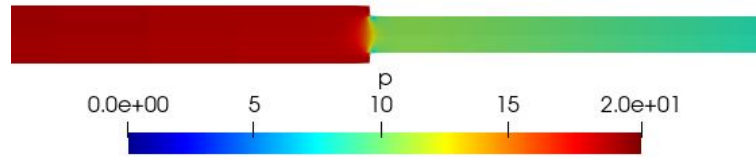


Figure 4.15: Pressure contour

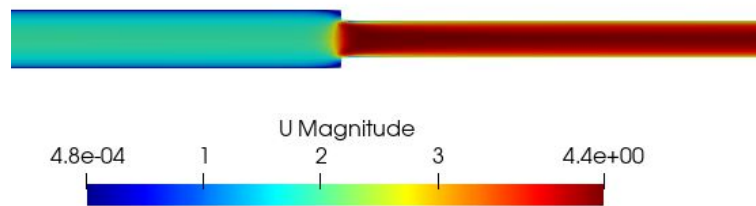


Figure 4.16: Velocity contour

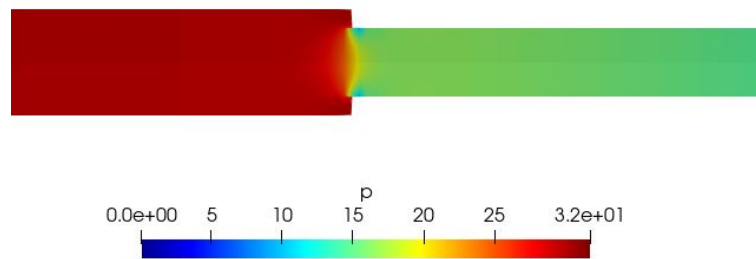


Figure 4.17: Pressure contour for Higher Reynolds number

4.2 Experimental Results

The experimental data was provided in the manual ?. The initial and final height of the collecting tank and the manometer's height difference was given. Using the

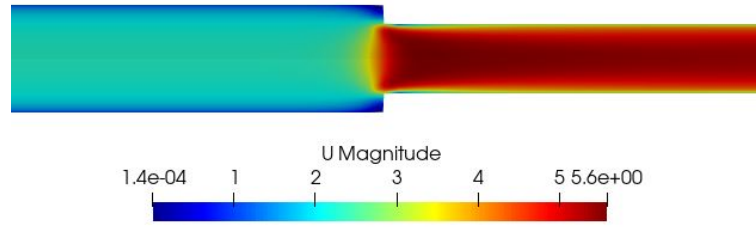


Figure 4.18: Velocity contour for Higher Reynolds number

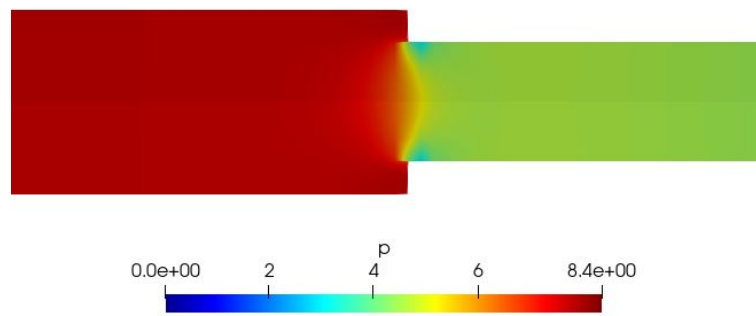


Figure 4.19: Pressure contour for Lower Reynolds number

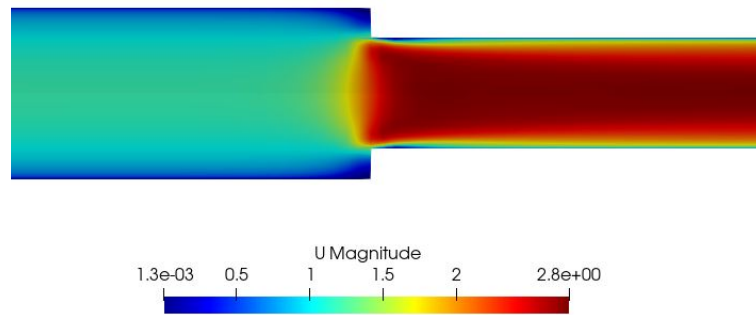


Figure 4.20: Velocity contour for Lower Reynolds number

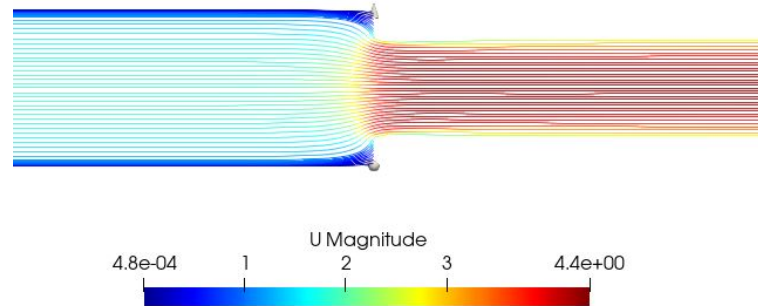


Figure 4.21: Streamlines with Velocity contour

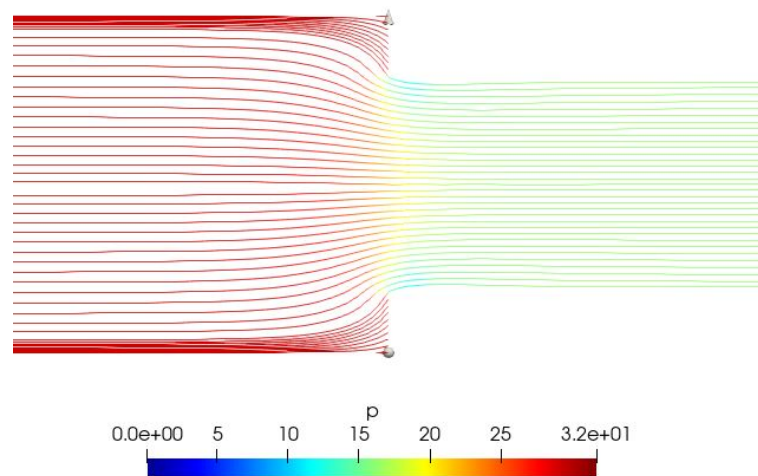


Figure 4.22: Streamlines with Velocity contour for Higher Reynolds number

collecting tanks reading, the flow rate was determined and the pressure head was determined using manometer's height difference. With Equation 1.3, the minor loss factor K for the experiment data was determined.

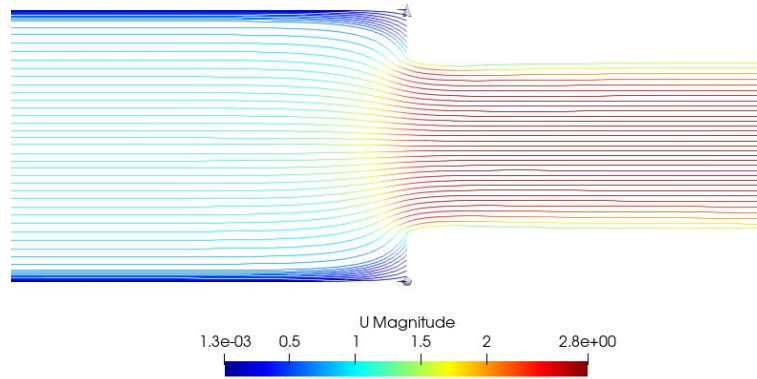


Figure 4.23: Streamlines with Velocity contour for Lower Reynolds number

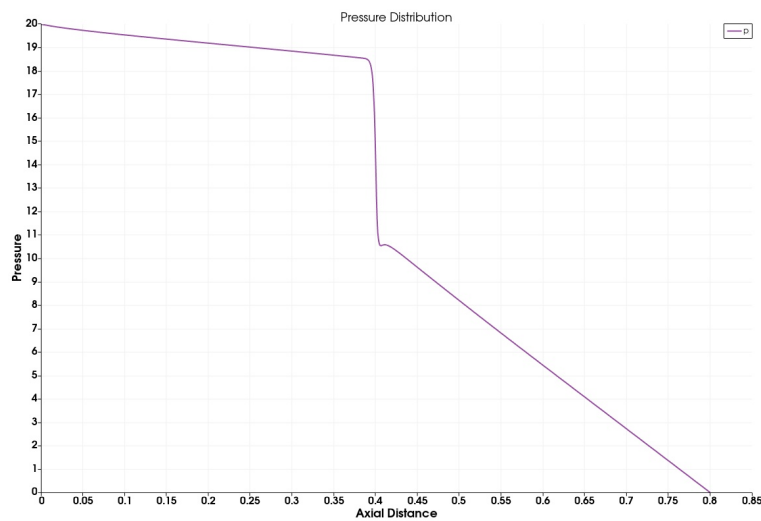


Figure 4.24: Pressure Distribution along the length

4.3 Result comparison

4.3.1 Sudden Expansion

The theoretical value for sudden expansion geometry was determined using the equation 4.1 and was determined to be equal to 0.3414.

$$K_{se} = \left(1 - \frac{d^2}{D^2}\right)^2 \quad (4.1)$$

Both the results obtained, CFD and experimental were compared and is summarised in the Table 4.1 with the input initial conditions for CFD simulations.

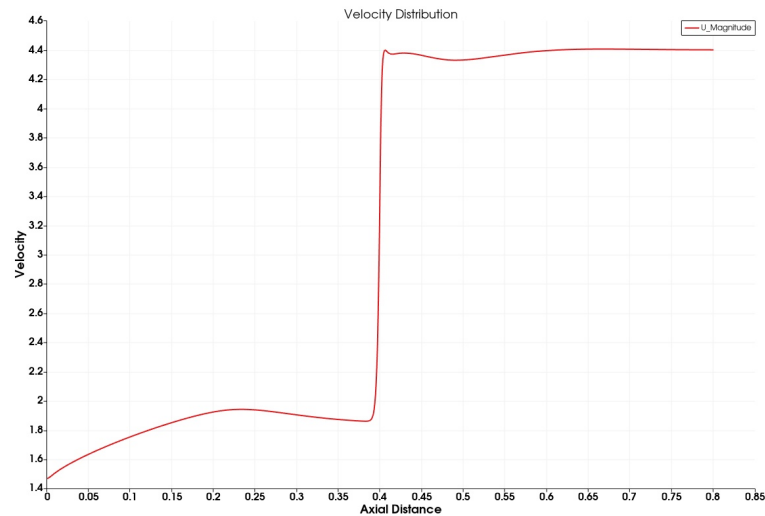


Figure 4.25: Velocity Distribution along the length

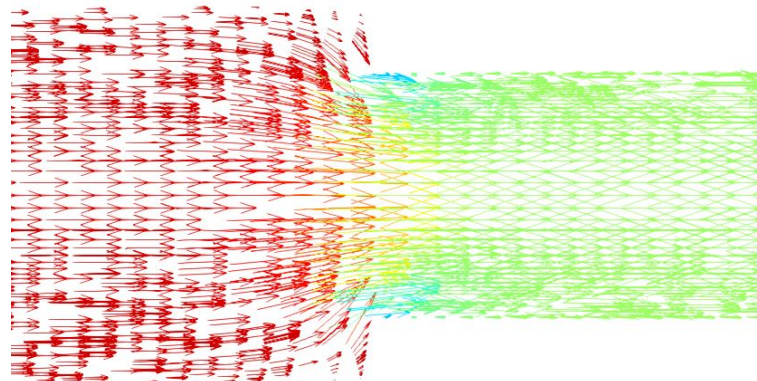


Figure 4.26: Vector plot for sudden contraction

4.3.2 Sudden Contraction

The analytical result for the given sudden contraction geometry was determined using the below equation,

$$K_{sc} = 0.42\left(1 - \frac{d^2}{D^2}\right) \quad (4.2)$$

Minor loss factor was determined only for the CFD simulations, as the loss factor from the experimental data gave a value greater than one. The values obtained are summarised in Table 4.2

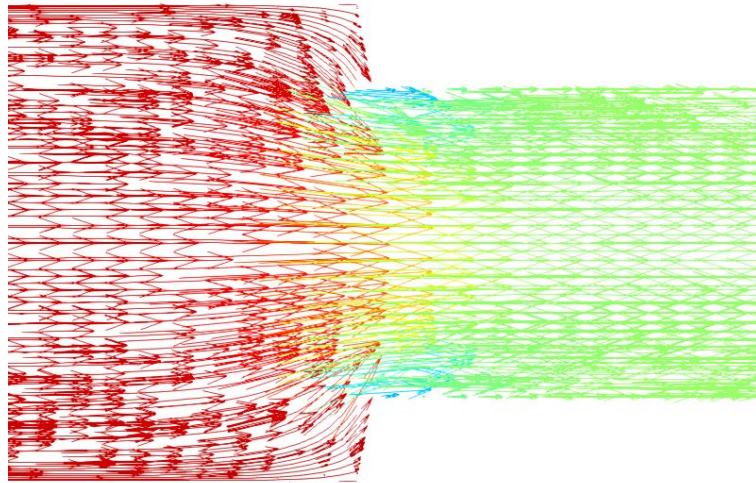


Figure 4.27: Vector plot for sudden contraction (High Reynolds number)

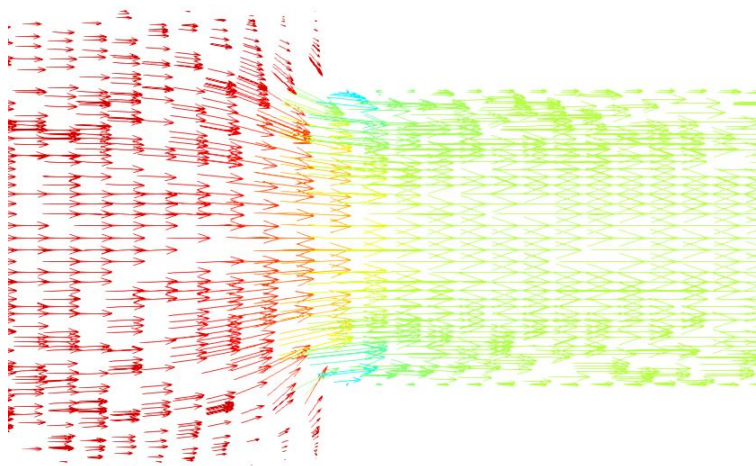


Figure 4.28: Vector plot for sudden contraction (Low Reynolds number)



Table 4.1: Experimental and CFD results for sudden expansion

Sl.No.	Flow rate(m^3/s)	Velocity (m/s)	Reynolds number	Turbulent kinetic energy (m^2/s^2)	Turbulent dissipation (m^2/s^3)	Pressure difference	K	K (exp)
1	0.000237261	3.553680534	32731	0.035935	1.7343	2.9593	0.4696	0.57622
2	0.000235939	3.533868651	32546.6	0.03553	1.7050	2.926	0.4686	0.638518
3	0.000202062	3.026465624	27903.408	0.027205	1.142	2.1416	0.4696	0.795926
4	0.0002099	3.143867317	28985.83	0.0289631	1.2508	2.3152	0.4696	0.569403
5	0.000194248	2.909425024	26824.668	0.025362	1.0283	1.9748	0.4696	0.607656
6	0.000181724	2.721851542	25078.4	0.022572	0.8632	1.7373	0.4696	0.444568
7	0.000300587	4.502156972	41490	0.0544	3.2303	4.7817	0.4722	0.646404
8	0.000293977	4.403161169	40568	0.0523	3.0451	4.5716	0.4722	0.637544
9	0.000282542	4.231889663	39000	0.04199	2.1906	4.2252	0.4722	0.717801
10	0.000277277	4.153026675	38263	0.04728	2.6173	4.0669	0.4722	0.630656
11	0.000287787	4.31044135	39738.2	0.05052	2.8909	4.3865	0.4722	0.705183
12	0.000290918	4.3573383	40107	0.05134	2.9616	4.4683	0.4722	0.390614
13	0.000104913	1.571377203	14475.4	0.008629	0.204	0.5788	0.4696	0.500586
14	0.000146918	2.200528707	20284	0.01557	0.4946	1.1365	0.4696	0.32163
15	9.87793E-05	1.479507415	13553.4	0.00769	0.1716	0.5074	0.4696	0.498051
16	0.000105852	1.585441164	14567.6	0.008725	0.2075	0.5862	0.4696	0.185879
17	6.28834E-05	0.941862287	8666.8	0.003516	0.053	0.2051	0.4642	0.351128



Table 4.2: Experimental and CFD results for sudden expansion

Sl No.	Flow rate(m^3/s)	Velocity (m/s)	Reynolds number	Turbulent kinetic energy (m^2/s^2)	Turbulent dissipation (m^2/s^3)	Pressure difference	K
1	0.000237	1.478038	21021	0.006858	0.09322	0.3024	0.2799
2	0.000236	1.469798	20878	0.0068	0.0922	0.2721	0.2553
3	0.000202	1.25876	17875	0.00518	0.0613	0.142	0.18176
4	0.00021	1.307589	18590	0.00555	0.068	0.2244	0.2656
5	0.000194	1.210081	17303	4.901e-3	0.0563	0.1056	0.1442
6	0.000182	1.132066	16159	4.348e-3	0.047	0.1576	0.2469
7	0.000301	1.872526	26741	0.0105	0.1766	0.5019	0.287
8	0.000294	1.831351	26169	0.0101	0.166	0.4884	0.2916
9	0.000283	1.760117	25168	9.4437e-3	0.1506	0.4663	0.301
10	0.000277	1.727316	24596	9.071e-3	0.1418	0.4468	0.3020
11	0.000288	1.792788	25597	9.727e-3	0.1574	0.4898	0.3057
12	0.000291	1.812293	25883	9.918e-3	0.1621	0.4812	0.2937
13	0.000105	0.653563	9345.05	1.65e-3	0.011	0.0604	0.286
14	0.000147	0.915238	13013	2.9772e-3	0.0266	0.1158	0.2799
15	9.88E-05	0.615353	8723	1.4785e-3	9.3321e-3	0.04411	0.237
16	0.000106	0.659413	9295	1.6523e-3	0.011	0.0547	0.2593
17	6.29E-05	0.391737	5577	6.7586e-4	2.8842e-3	0.01096	0.1442

Chapter 5

Conclusion

In this case study, simulation of turbulent flow through sudden expansion and contraction was done using $\kappa - \epsilon$ RANS turbulence model. The minor loss factor was determined for both the cases in Reynolds number range of 5500-40000. The obtained minor loss factor was compared with theoretical and experimentally obtained values. Velocity, pressure contours and streamlines were visualised through which various distinctive flow behaviours were studied.